Protoplasma (2010) 243:95–103
DOI 10.1007/s00709-009-0064-5

ORIGINAL ARTICLE

PAR modulation of the UV-dependent levels of flavonoid metabolites in *Arabidopsis thaliana* (L.) Heynh. leaf rosettes: cumulative effects after a whole vegetative growth period

Michael Götz · Andreas Albert · Susanne Stich · Werner Heller · Hagen Scherb · Andreas Krins · Christian Langebartels · Harald K. Seidlitz · Dieter Ernst

Received: 19 January 2009 / Accepted: 13 July 2009 / Published online: 12 August 2009

Abstract Long-term effects of ultraviolet (UV) radiation on flavonoid biosynthesis were investigated in *Arabidopsis thaliana* using the sun simulators of the Helmholtz Zentrum München. The plants, which are widely used as a model system, were grown (1) at high photosynthetically active radiation (PAR; 1,310 μmol $m^{-2}s^{-1}$) and high biologically effective UV irradiation (UV-B_{BE} 180 mW m^{-2}) during a whole vegetative growth period. Under this irradiation regime, the levels of quercetin products were distinctively elevated with increasing UV-B irradiance. (2) Cultivation at high PAR (1,270 μmol $m^{-2}s^{-1}$) and low UV-B (UV-B_{BE} 25 mW m^{-2}) resulted in somewhat lower levels of quercetin products compared to the high-UV-B_{BE} conditions, and only a slight increase with increasing UV-B irradiance was observed. On the other hand, when the plants were grown (3) at low PAR (540 μmol $m^{-2}s^{-1}$) and high UV-B (UV-B_{BE} 180 mW m^{-2}), the accumulation of quercetin products strongly increased from very low levels with increasing amounts of UV-B but the accumulation of kaempferol derivatives and sinapoyl glucose was less pronounced. We conclude (4) that the accumulation of quercetin products triggered by PAR leads to a basic UV protection that is further increased by UV-B radiation. Based on our data, (5) a combined effect of PAR and different spectral sections of UV radiation is satisfactorily described by a biological weighting function, which again emphasizes the additional role of UV-A (315–400 nm) in UV action on *A. thaliana*.

Keywords *Arabidopsis thaliana* · Biological weighting function (BWF) · Flavonoids · Quercetin derivatives · Photosynthetically active radiation (PAR) · Ultraviolet (UV)-B radiation

Dedicated to Professor Cornelius Lütz on the occasion of his 65th birthday

Electronic supplementary material The online version of this article (doi:10.1007/s00709-009-0064-5) contains supplementary material, which is available to authorized users.

M. Götz · S. Stich · W. Heller · C. Langebartels · D. Ernst (✉)
Institute of Biochemical Plant Pathology, Helmholtz Zentrum München—German Research Center for Environmental Health, 85764 Neuherberg, Germany
e-mail: ernst@helmholtz-muenchen.de

A. Albert · A. Krins · H. K. Seidlitz
Department of Environmental Engineering, Helmholtz Zentrum München—German Research Center for Environmental Health, 85764 Neuherberg, Germany

H. Scherb
Helmholtz Zentrum München—German Research Center for Environmental Health, Institute of Biomathematics and Biometry, 85764 Neuherberg, Germany

Present Address:
M. Götz
Breun Seeds GdbR,
91074 Herzogenaurach, Germany

Introduction

A decline in stratospheric ozone concentrations with a concomitant increase of ultraviolet (UV)-B radiation (280–315 nm) reaching the Earth's surface has occurred during recent decades. This effect is thought to be caused by human activities. Furthermore, it is still under debate whether and, if so, when the ozone layer will recover to levels measured before 1980. It has to be kept in mind that the recovery will occur in an atmosphere that has also changed considerably since 1980 due to global warming (McKenzie et al. 2007; Weatherhead and Andersen 2006). Damaging effects on organisms by enhanced UV-B radiation equivalent to relatively high ozone depletion rates

have been extensively described (see review by Caldwell et al. 2007). Changes in UV-B irradiation are not only related to its intensity but also to its spectral composition, i.e., increasing shortwave (<300 nm) energy-rich components.

UV-B radiation has the potential to jeopardize genome stability and the functionality of cellular components, such as DNA, proteins, and lipids (Jordan 1996; Mazza et al. 1999; Ries et al. 2000; Stapleton 1992). Thus, it can modify, or even impair, physiological processes, which may affect plant growth (Bornman and Teramura 1993; Jansen et al. 1998).

A well-known protective mechanism against UV-B radiation in plants is the formation of UV-B screening pigments (Jordan 1996; Langebartels et al. 2002). Flavonoids and soluble hydroxycinnamic acid derivatives, in particular catechol-type structures, seem to be most efficient, as has been demonstrated for several plant species (Burchard et al. 2000; Ibdah et al. 2002; Schnitzler et al. 1996; Ryan et al. 1998, 2001). However, effects upon long-term UV-B irradiation on plants were often not adequately studied or quantified (Casati and Walbot 2003; Giordano et al. 2003; Izaguirre et al. 2003; Rousseaux et al. 1999; Schnitzler et al. 1999). Several long-term studies with flavonoid mutants and transgenic plants further support the essential role of UV-B absorbing pigments (Bieza and Lois 2001; Ryan et al. 2002).

The importance of taking both photosynthetically active radiation (PAR) and UV-A radiation into account in understanding plant responses to elevated UV-B radiation was recently noted (Berkelaar et al. 1994; Caldwell et al. 2007; Cooley et al. 2000; Krizek 2004; Yao et al. 2006). As PAR and UV-A radiation are not affected by atmospheric ozone absorption, their intensity ratio remains almost constant, whereas the ratio of UV-B to PAR strongly depends on the actual ozone column being penetrated, which exhibits a diurnal course. Experiments specifically designed to study the interaction of all spectral bands in sunlight should therefore include a scenario with a typical natural UV-B to PAR ratio (Caldwell and Flint 1994). A typical noon value of this ratio during a midlatitude summer is 1:290 when taken on the basis of energetic weighting over the respective spectral bands (see also caption of Table 1).

High-PAR intensities have more recently been recognized to modify changes in gene expression and the accumulation of phenylpropanoids induced by UV-B radiation (Ibdah et al. 2002; Kaffarnik et al. 2006; Rossel et al. 2002). We have earlier shown that mesembryanthin, the major flavonol derivative in *Mesembryanthemum crystallinum* L., accumulated in a spectrally dependent manner upon UV-B irradiation (Ibdah et al. 2002). Furthermore, several light-stress-regulated genes have been characterized in detached mature leaves of *Arabidopsis thaliana* exposed to a PAR value of 2,500 µmol $m^{-2}s^{-1}$ for 2 h using differential display techniques (Dunaeva and Adamska 2001). Changes in gene expression after moving *A. thaliana* plants from a PAR exposure of 100 to 1,000 µmol $m^{-2}s^{-1}$ have also been reported (Rossel et al. 2002). In another long-term exposure experiment with *A. thaliana* at PAR conditions of about 1,000 µmol $m^{-2}s^{-1}$, UV-B regulation of P450 monooxygenases, glucosyltransferases, and glutathione transferases was described (Glombitza et al. 2004).

UV-A radiation and blue light play a key role in the photorepair of DNA damage caused by UV-B exposure (Sancar 1994). However, little is known on the interaction of various UV components and PAR. Although the borderline between UV-A and UV-B is clearly set by definition, the plant's response to both cannot easily be disentangled in the transitional range between approximately 310 and 330 nm. The present study now focuses on effects of different UV-B/UV-A regimes and PAR intensities on the levels of relevant UV-B-absorbing metabolites.

Table 1 Integrated PAR given as photosynthetic photon flux density, biologically effective irradiance UV-B_{BE} normalized at 300 nm according to Caldwell (1971) and energetic weighted[a] UV-B, UV-A, and PAR irradiances of the different exposures

PAR/UV scenario Irradiance	High/high	Low/high	High/low
Under all filters			
PAR (µmol $m^{-2}s^{-1}$)	1,310	540	1,270
PAR (W m^{-2})[a]	285	117	276
Filter slots WG 295, 305			
UV-A (W m^{-2})[a]	31	16	23
Filter slot WG 320			
UV-A (W m^{-2})[a]	28	12	22
Filter slot WG 335			
UV-A (W m^{-2})[a]	24	10	19
Filter slot WG 360			
UV-A (W m^{-2})[a]	14	5	13
Filter slot WG 295			
$UV\text{-}B_{BE}$ (mW m^{-2})	180	180	25
UV-B (W m^{-2})[a]	1	1	0.14
UV-B/PAR ratio[a]	1:285	1:117	≈1:2,000
Filter slot WG 305			
$UV\text{-}B_{BE}$ (mW m^{-2})	150	130	20
Filter slots WG 320, 335, 360			
$UV\text{-}B_{BE}$ (mW m^{-2})	<1.5	<1.5	<1.5

The values represent the average of two experiments for each PAR/UV scenario with similar irradiation and climate conditions. In addition, PAR is averaged over the five slots of the cuvette. Uncertainties of irradiance measurements are approximately ±8%.

[a] The term "energetic" weighting means that the spectral irradiance is simply integrated over the respective spectral band. E.g., the UV-B/PAR ratio of natural terrestrial solar radiation during a midlatitude summer under clear sky yields an approximate noon value of ≈1:290, where [UV-B] = 1.5 Wm^{-2} and [PAR] = 440 Wm^{-2} is used.

We analyzed flavonol and sinapic acid products in leaf rosettes of *A. thaliana* grown for 14 days under different PAR/UV-B regimes. Our results demonstrate that, in the long run, UV-B effects were highly significant at low-PAR and high-UV-B radiation and also with high-PAR and high-UV-B radiation but not so concisely at high-PAR and low-UV-B radiation. The accumulation data, particularly of quercetin derivatives, were used to derive a biological weighting function (BWF) in order to describe the spectral dependence of their formation and its modulation by PAR.

The present experiments showed that the plants' natural response to chronic exposure of high-PAR irradiance together with UV irradiation can only be observed under a UV/PAR spectral balance close to that of sunlight.

Materials and methods

Simulation of UV radiation

A sun simulator of the Helmholtz Zentrum München was used for the application of polychromatic irradiation regimes (Thiel et al. 1996). A temperature- and humidity-controlled cuvette integrated into the sun simulator was subdivided into five separate compartments covered by the five different cutoff filters WG 295, WG 305, WG 320, WG 335, and WG 360 to obtain different proportions of UV-B and UV-A radiation (Schott, Mainz, Germany; see also graphical contents entry). Light and UV radiation conditions, as well as the control of air and soil temperature have recently been described (Ibdah et al. 2002). The spectroradiometric assessment of UV and PAR was performed using a double monochromator system (Bentham D300, Reading, UK) and a calibration lamp (Gigahertz, Puchheim, Germany), the calibration of which can be traced back to the Physikalisch-Technische Bundesanstalt, Braunschweig, Germany (German National Bureau of Standards). The three irradiation scenarios, each representing defined PAR and UV-B_{BE} values, were replicated under comparable conditions, permitting an evaluation of 30 irradiation variations. The scenario of high PAR/high UV-B_{BE} was especially designed to form a realistic UV-B/PAR ratio under the WG 295 filter. The corresponding spectral data are summarized in Table 1.

Plant material

A. thaliana Col 0 (Lehle, Nottingham, UK) was cultivated on standard soil (type Floraton; Bayerische Gärtnerei-Genossenschaft, München, Germany), mixed with 1/16 volume of sterile sand (Ø 0.1–0.4 mm) and the same volume quartz sand (Ø 0.6–1.2 mm; Dorfner, Hirschau, Germany). Three seeds each were applied to five positions per cultivation pot (6×6 cm, TEKU multifilter palettes PL2838/24, Pöppelmann, Lohne, Germany). Pots were pretreated at 4°C for 2 days in the dark, then transferred to the sun simulator, where they were kept at PAR values of 200 µmol $m^{-2}s^{-1}$ under the exclusion of UV radiation (<400 nm), 14/10 h day/night cycles and an average temperature of 20°C. Germination occurred within 4 days. The number of plants per cultivation pot was reduced to five on day 9. PAR and UV treatments according to the scenarios listed in Table 1 started on day 11 upon removing the UV exclusion filter. The PAR/UV exposure occurred for 14/12 h per day, and the UV treatment was started 1 h after onset of PAR. Leaf rosettes were harvested after a 14-day irradiation period beginning at 1400 hours Central European Time in all experiments. Plants grown under a defined WG filter were pooled as follows: the leaf rosettes of two to four cultivation pots were combined, resulting in three sample pools each consisting of ten to 20 rosettes. Plant material was frozen in liquid nitrogen and stored at −80°C until further analysis.

HPLC analysis

High-performance liquid chromatography (HPLC) separation of soluble metabolites was performed according to the procedure of Turunen et al. (1999), using a 250×4.6 mm Spherisorb ODS2 5.0-µm column (Bischoff, Leonberg, Germany). Samples (methanol–water, 75:25, *v*/*v*, injection volume 10 µl) were eluted from the column using a solvent gradient starting with solvent A [980 ml H_2O+20 ml 5% ammonium formate in formic acid (98 %)] and adding increasing amounts of solvent B [882 ml methanol (HPLC grade) + 96 ml H_2O + 20 ml 5% ammonium formate in formic acid (98%)]. The gradient was as follows: 0–5 min 0% B; 5–45 min 0–100 % B (linear); 45–48 min 100% B; 48–50 min 100–0% B; and 50–58 min 0% B. The eluent was monitored at 280 nm with a UV/visible diode array detector (Beckman Coulter, Krefeld, Germany) followed by an in-line spectrofluorimeter (excitation at 300 nm, emission at 400 nm; Shimadzu Model RF530, Duisburg, Germany). Metabolite levels were determined as nanomole equivalents per milligram FW based on the reference compounds kaempferol 3-*O*-rhamnoside (Afzelin) for kaempferol derivatives and quercetin 3-*O*-rhamnoside (Quercitrin) for quercetin derivatives, both from Apin Chemicals Ltd., Oxon, UK, and methyl sinapate synthesized from sinapic acid for sinapic acid esters (Fluka, Buchs, Switzerland). Products were assigned according to their characteristic diode array spectra. No myricetin derivatives have so far been detected in the *A. thaliana* WT Col-0 under our conditions. Leaf area-related concentrations were calculated using the experimentally determined factor 23.7 mg cm^{-2}. This transformation allows a direct comparison with fluence data. Sample chromatograms of the HPLC analyses are given in Fig. 1.

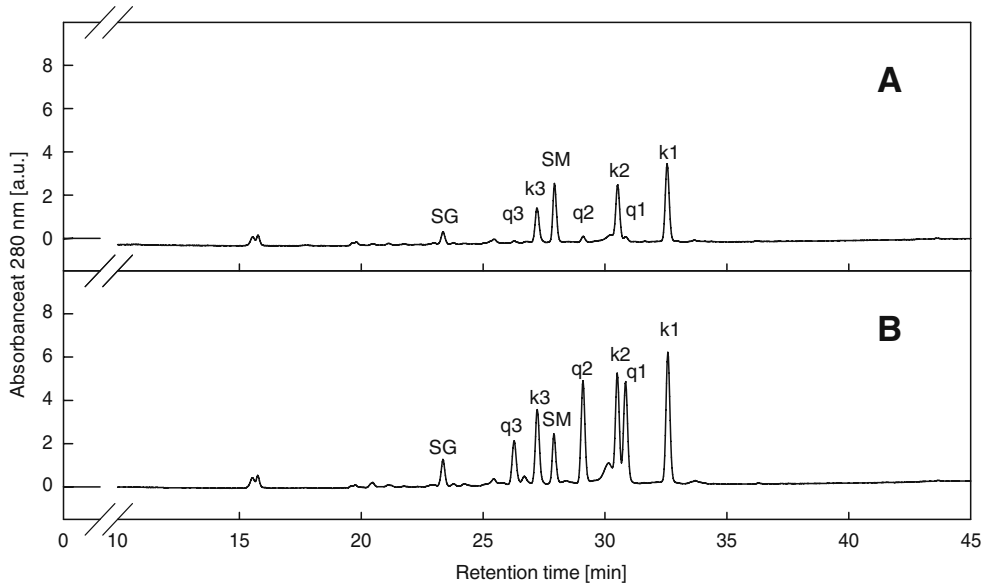

Fig. 1 Typical HPLC diagrams of flavonol and sinapic acid metabolites from *A. thaliana* leaf rosettes exposed to low-PAR/high-UV irradiation conditions (compare Fig. 2). **A** Under exclusion of UV-B radiation (WG 360), reasonable amounts for sinapic acid (*SG* and *SM*) and kaempferol (*k1–k3*) derivatives are observed. Only very minor signals appear for the respective quercetin derivatives (*q1–q3*). **B** In the presence of UV-B radiation (WG 305), quercetin derivatives (*q1–q3*) are strongly induced, while sinapoyl glucose (*SG*) and the kaempferol derivatives (*k1–k3*) are only slightly elevated, while sinapoyl malate (SM) is not affected at all. A third sinapic acid derivative cannot be observed in these chromatograms

Results and discussion

In order to test a possible long-term regulation of flavonol and sinapic acid biosynthesis in *A. thaliana* leaf rosettes under continuous UV-B irradiation regimes, we focused on the most prominent accumulation of quercetin derivatives. Typical HPLC diagrams for metabolite extracts from a sample of one of the two low-PAR high-UV experiments are shown in Fig. 1. The irradiation regimes are described in the "Materials and methods" section, and the numerical values are listed in Table 1. The high-UV regime was applied at two different PAR conditions (*approximately* 1,300 and 540 µmol $m^{-2}s^{-1}$). A third experiment was performed at high PAR and reduced low levels of UV irradiance using the filter set mentioned above.

Experiments performed under the high-PAR and high-UV-B regime (PAR 1,310 µmol $m^{-2}s^{-1}$ and UV-B_{BE} up to 180 mW m^{-2})

Growth of *A. thaliana* under the high-PAR/high-UV-B_{BE} regime resulted in the most prominent accumulation of quercetin derivatives in the leaf rosettes (Fig. 2) and occurred increasingly in a spectral-dependent manner with decreasing UV wavelengths. A similar behavior has been found in *M. crystallinum* for levels of flavonol and betacyanin metabolites with *ortho*-dioxy structures (Ibdah et al. 2002). Accumulation of related UV-B-absorbing compounds has also been described for UV-B-exposed field-grown barley (Mazza et al. 1999) as well as *Vicia faba* L. (Meijkamp et al. 2001). Exclusively, kaempferol-derived flavonol metabolites were found in F3′H-deficient mutant *Petunia hybrida ht1* under any irradiation condition (Ryan et al. 2002). It has been shown that these plants were less resistant towards UV-B-damaging processes, underlining the crucial function of quercetin derivatives in the UV-B protection mechanism and indicating an antioxidant component in this process. Similarly, *A. thaliana tt7* mutants, which do not contain quercetin derivatives, are more susceptible to UV-B irradiation than to the wild-type line. This again indicates that kaempferol is not as efficient as quercetin in UV-B protection (Ryan et al. 2001). Even in the absence of UV-B radiation, a certain level of quercetin derivatives exists, demonstrating the importance of high light intensities. Additional experiments with cutoff filters GG 400 and GG 420 that block UV-A completely while leaving PAR almost unaltered still showed a basal level of quercetin derivatives at an average of 50 nmol cm^{-2}, which could be accounted for solely by the influence of at least the blue light component of PAR.

Experiments performed under the low-PAR and high-UV-B regime (PAR 540 µmol $m^{-2}s^{-1}$ and UV-B_{BE} up to 180 mW m^{-2})

To further highlight the role of PAR values in the modulation of plant responses to UV-B radiation, additional comparisons were performed with a low-PAR/high-UV-B_{BE}

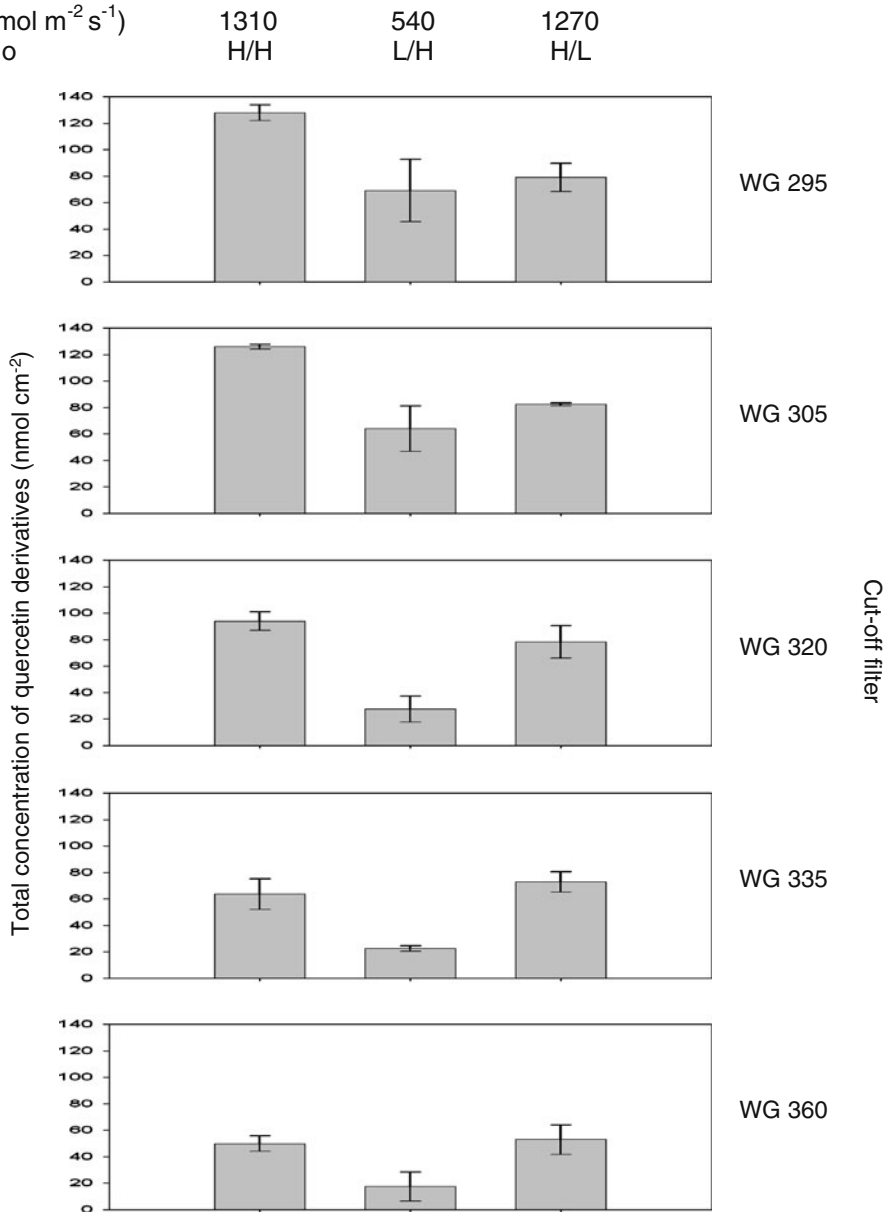

Fig. 2 Effects of PAR and UV-B radiation on the accumulation of quercetin derivatives. *A. thaliana* were analyzed after 14 days of growth under the irradiation conditions given as high PAR/high UV-B H/H, low PAR/high UV-B L/H, and high PAR/low UV-B H/L. The *bars* represent the average data obtained from two experiments under each scenario with the corresponding standard deviations. Analysis of variance resulted in significant differences of high PAR/high UV-B and high PAR/low UV-B vs. low PAR/high UV-B but not of high PAR/high UV-B vs. high PAR/low UV-B. However, all three regressions are significant. Mathematical calculations and regressions are given in "Electronic Supplementary Material"

regime. The quercetin derivatives again accumulated in a spectral-dependent manner under the low-PAR/high-UV-B_{BE} scenario, although the absolute amounts were significantly lower than in the high-PAR/high-UV-B_{BE} scenario (Fig. 2). These data further underline the influence of high PAR in addition to high UV-B_{BE} in the accumulation of quercetin derivatives.

Experiments performed under the high-PAR and low-UV-B regime (PAR 1,270 µmol $m^{-2}s^{-1}$ and UV-B_{BE} up to 25 mW m^{-2})

When we analyzed the effect of high PAR and overall reduced UV radiation (high PAR/low UV-B_{BE}), the amount of quercetin derivatives showed no prominent increase with decreasing UV wavelength under this regime, and nearly constant levels were found in the range of 60–70 nmol cm^{-2} (Fig. 2).

Effects of UV irradiation on kaempferol and sinapic acid derivatives

In addition to quercetin derivatives, we analyzed kaempferol and sinapic acid metabolites. Under the high-PAR/high-UV-B_{BE} regime, we observed a weak spectral dependence only for the accumulation of kaempferol derivatives (*k1–k3*) and sinapoyl glucose (see Fig. 1; detailed data not shown). Two further sinapic acid derivatives, sinapoyl malate and an additional minuscule metabolite, did not show any measurable spectral dependence. This suggests a

constitutive UV protection effect for these metabolites that is less affected by PAR and, in particular, UV-B irradiation under any condition of our experiments. However, it cannot be excluded that these metabolites may play a protective role in specific minor compartments or that their biosynthesis may be affected under other conditions, e.g., transient induction processes.

Biological weighting function (BWF)

The description of the mathematical analysis to develop a BWF from the set of experimental data is similar to that described by Ibdah et al. (2002). Based on the broad data set obtained from the metabolite analyses of plants exposed under the five WG filter types, a BWF describing the spectral dependence of the most strongly UV-induced quercetin metabolites in *A. thaliana* Col 0 at 20°C was developed:

In order to investigate the spectral dependence of the accumulation of the quercetin derivatives, q_{measured}, in the ultraviolet (UV) range of the spectrum, the influence of the accompanying PAR has to be separated from the combined effect of UV and PAR. Under the WG 360 filter, PAR only contributes to the formation of quercetin derivatives in the leaf rosettes (Fig. 2). These concentration values, q_{PAR}, obtained from plants grown under the WG 360 filter in our six different experiments were considered to be proportional to the PAR irradiance E_{PAR}, and the regression analysis of our data points yielded

$$q_{\mathrm{PAR}} = 0.043 \left[\frac{\mathrm{nmol\ cm^{-2}}}{\mu\mathrm{mol\ m^{-2}s^{-1}}}\right] \cdot E_{\mathrm{PAR}}\left[\mu\mathrm{mol\ m^{-2}s^{-1}}\right] \quad (1)$$

with a correlation coefficient of r=0.88. Using this basal value induced by PAR only, we calculated the net UV-induced concentration of quercetin derivatives, $q_{\mathrm{UV}} = q_{\mathrm{measured}} - q_{\mathrm{PAR}}$, for each scenario and spectrum. Negative values were interpreted as zero.

From these net data, the BWF, $s(\lambda)$, for the UV-dependent accumulation of quercetin derivatives in leaf rosettes of *A. thaliana* under chronic exposure conditions was determined. This BWF is not directly accessible from the data because the UV-induced concentrations of quercetin derivatives result from the simultaneous action of two quantities, the spectral dependence itself and the dose function $W(H_{\mathrm{BA}})$. Therefore, a numerical analysis and mathematical interpretation of the net data are required. The model of evaluation is that the (physical) spectral radiant exposures are weighted with the BWF $s(\lambda)$, and integration over all wavelengths gives H_{BA}, where H_{BA} is the biologically effective radiant exposure. The measured UV-induced concentrations of quercetin derivatives are then determined from the dose function, which only depends on H_{BA}. Due to the limited number of spectra combined with a rather large experimental biological variability, only elementary assumptions on the shape of the BWF and on the dose function are made:

(a) A monoexponential function was set up to describe the wavelength dependence of $s(\lambda)$:

$$s(\lambda) = \exp[-k \cdot (\lambda - \lambda_0)]. \quad (2)$$

The BWF was normalized to unity at $\lambda=\lambda_0$=300 nm in order to allow a comparison with other BWFs. The slope parameter k has to be determined.

(b) Using this BWF, the biologically effective UV dose (effective radiant exposure) H_{BA} is given by

$$\begin{aligned} H_{\mathrm{BA}} &= \int \mathrm{d}t \cdot \mathrm{d}\lambda \cdot s(\lambda) \cdot E_\lambda(\lambda, t) \\ &= \int \mathrm{d}\lambda \cdot s(\lambda) \cdot H_\lambda(\lambda) \end{aligned} \quad (3)$$

$E_\lambda(\lambda,t)$ is the spectral irradiance (see Fig. 3 for example), and $H_\lambda(\lambda)$ is the corresponding spectral radiant exposure.

(c) The dose function $W(H_{\mathrm{BA}})$ correlates the biologically effective UV dose, H_{BA}, with the measured UV-induced concentrations of quercetin derivatives, q_{UV}. For simplicity, the concentration of quercetin derivatives was assumed to be proportional to H_{BA}:

$$q_{\mathrm{UV}} = W(H_{\mathrm{BA}}) = w \cdot H_{\mathrm{BA}} \quad (4)$$

The slope, w, of the dose function has to be determined.

The calculation of the BWF is thus based on the estimation of the parameters k and w. The reasonable range

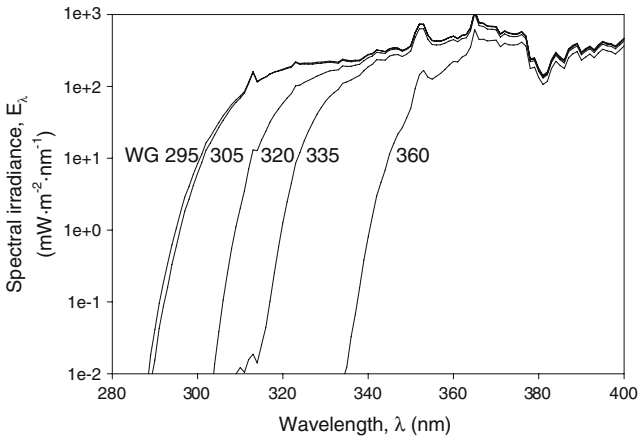

Fig. 3 Spectral irradiances E_λ within the five slots of the cuvette at the scenario high PAR/high UV with cutoff filters WG 295, 305, 320, 335, and 360

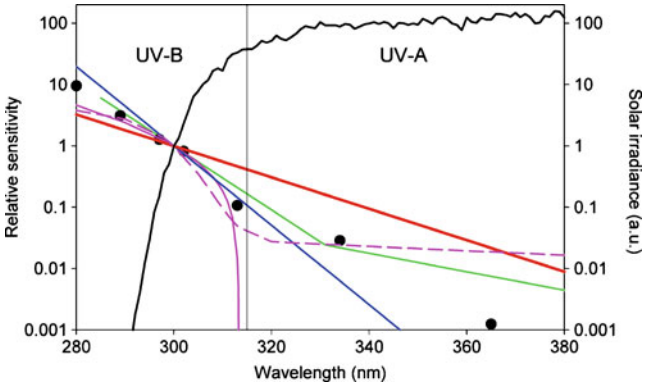

Fig. 4 Logarithmic plot of biological weighting functions obtained from this work and from the literature together with a typical solar midday spectrum: induction of quercetin derivatives in *A. thaliana* (*solid red line*; this work). Generalized plant action spectrum (*solid magenta line*; Caldwell 1971). Modified plant action spectrum (*dashed magenta line*; Flint and Caldwell 2003). Mesembryanthin accumulation in *M. crystallinum* (*solid blue line*; Ibdah et al. 2002). Inhibition of photosynthesis in *D. salina* (Ghetti et al. 1999). DNA damage in alfalfa (*full circles*; Quaite et al. 1992). Terrestrial solar midday spectrum measured on April 17th 1996 at 48.22° N, 11.60° E, 495 m above sea level, no clouds, solar elevation 52°, mean total ozone column 320DU (*solid black line*)

of parameter values was roughly determined to be within the boundaries of

$$k \in \left[1\ \mu\mathrm{m}^{-1}, 500\ \mu\mathrm{m}^{-1}\right]$$

and

$$w \in \left[0.001\frac{\mathrm{nmol\ cm}^{-2}}{\mathrm{J\,m}^{-2}},\ \ 1,000\frac{\mathrm{nmol\ cm}^{-2}}{\mathrm{J\,m}^{-2}}\right].$$

Optimization of the parameters was done using the SOLVER macro of Microsoft EXCEL® and yielded

$$k = 59\ \mu\mathrm{m}^{-1} \text{ and}$$

$$w = 0.65\frac{\mathrm{nmol\ cm}^{-2}}{\mathrm{J\,m}^{-2}}$$

for an UV irradiance exposure of 12 h in our experiments. The result, a monoexponential curve (Eq. 2), is depicted in Fig. 4 (solid red line) together with other BWFs from the literature. All spectra were normalized at 300 nm. A typical terrestrial solar UV spectrum is also presented for comparison (Fig. 4). Apart from the curve with the steep decay at

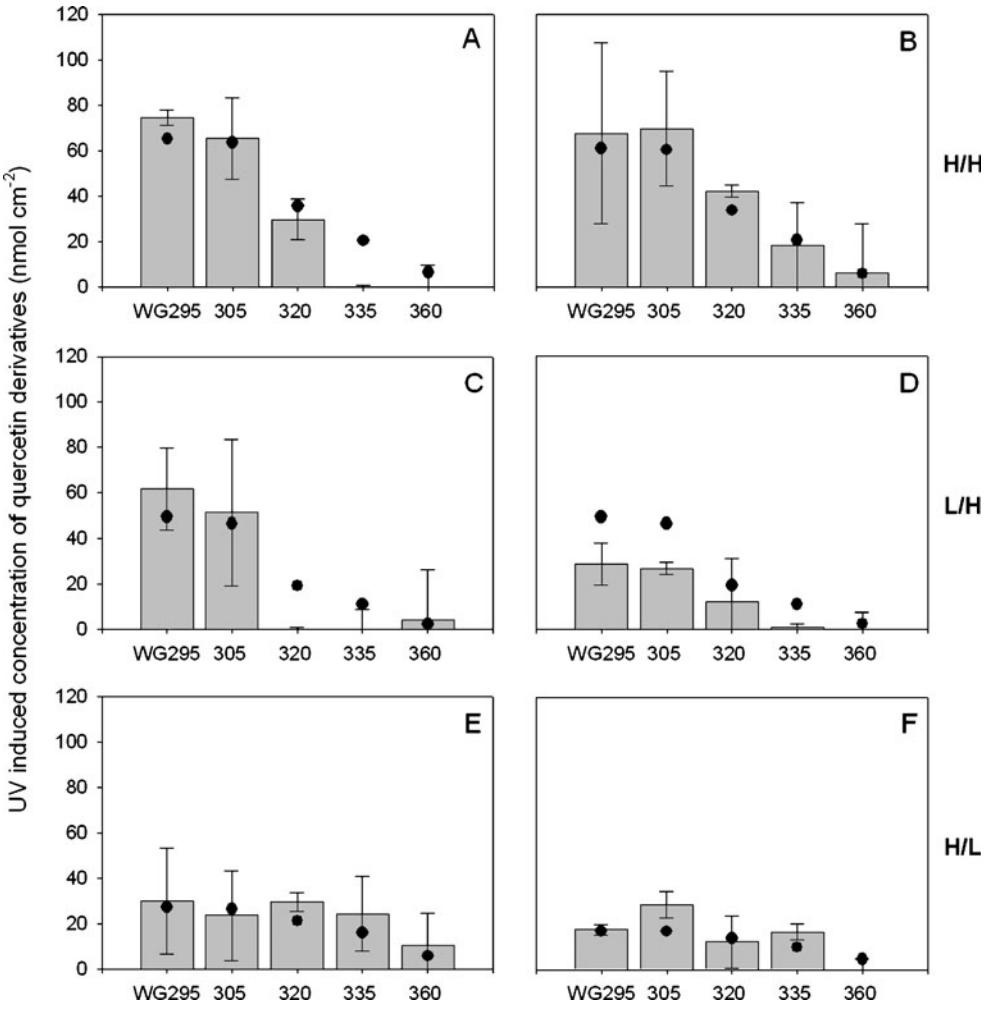

Fig. 5 Comparison of experimental data obtained for concentrations of quercetin derivatives and mathematical model data. *Gray bars* show the net UV-induced concentration of quercetin derivatives adjusted by subtraction of the PAR basic value (see text) together with the respective standard error, from three experiments (*left column*, **A**, **C**, and **E**) and the three respective replicates (*right column*, **B**, **D**, and **F**). *Full circles* represent the concentration as calculated from the BWF shown in Fig. 4. Scenarios: *H*/*H*, high PAR/high UV-B; *L*/*H*, low PAR/high UV-B; *H*/*L*, high PAR/low UV-B

313 nm, earlier denoted as the "generalized plant action spectrum" (magenta solid line after Caldwell 1971), on which the UV-B_{BE} data given in the literature and in this work are calculated, the spectra exhibit sensitivity in the UV-A range. So does also a more recent modification of the generalized plant action spectrum (dashed magenta line after Flint and Caldwell 2003).

In view of the large uncertainty in determining BWFs, especially when dealing with intact plants interacting with additional environmental factors, we conclude that the different slopes between the remaining curves in Fig. 4, DNA damage in alfalfa (full black circles after Quaite et al. 1992), inhibition of photosynthesis in *Dunaliella salina* (SAG 19-3; solid green line after Ghetti et al. 1999), mesembryanthin accumulation in *M. crystallinum* (solid blue line after Ibdah et al. 2002), and the present one for quercetin formation in *A. thaliana*, are probably not significant.

The spectral overlap between the solar spectrum and most BWFs shown in Fig. 4 underlines the important role of the UV-A domain of sunlight in regulating the plant's UV response. The lower sensitivity is compensated for by higher intensities of solar radiation in the UV-A range, where ozone absorption is of low importance compared to the UV-B component. We therefore suggest that the possible implication of UV-A should gain more attention in studies on UV effects, particularly in plants. This was also suggested recently for field-grown barley and soybean cultivars (Sullivan et al. 2007).

Using the optimal fit parameters k, w, the spectral irradiance $E_\lambda(\lambda,t)$ measured with our double monochromator system and Eqs. 2, 3, and 4, we calculated the UV-induced concentration, $q_{UV,\ model}$, shown in Fig. 5 as full circles. As mentioned previously, PAR-only exposure produced a base amount of quercetin derivatives in the long run. Therefore, the experimental values of quercetin accumulation (Fig. 5, gray bars) for all individual experiments were adjusted by subtraction of the basal value, which is obtained from the model (Eq. 1). The regression analysis of experimental and modeled data yielded a maximum difference in slope of less than 10% with a correlation coefficient r=0.91. As only five of 30 modeled data points in Fig. 5 lie slightly outside the uncertainty margins of the experimental data, we are quite confident about the validity of our BWF for the UV induction of quercetin derivatives in *A. thaliana*.

Conclusions

The experiments presented here were devised to provide a better understanding of plant performance under natural radiation regimes with prolonged UV-B exposure. Our data clearly demonstrate that PAR values up to 1,300 μmol $m^{-2}s^{-1}$ come closer to natural high light conditions than any others used so far when dealing with intact plants (Berkelaar et al. 1994). Moreover, we found that even values of approximately 500 μmol $m^{-2}s^{-1}$ still represent rather moderate light conditions. Therefore, experiments performed under PAR values less than 500 μmol $m^{-2}s^{-1}$ cannot be considered to be "high-PAR" studies. However, these conditions might be valuable for studying plant behavior under shaded germination conditions as well as for mechanistic investigations. Our experiments showed that the chronic application of realistic high-PAR irradiance together with UV irradiation conditions as encountered in the field is an important prerequisite for the observation of natural plant behavior.

Under these premises, our data indicate that, apart from UV-B radiation, the induction of quercetin derivatives in *A. thaliana* leaf rosettes is also influenced by UV-A radiation and strongly coregulated by PAR. It was shown that induction of secondary metabolites by PAR may provide a basic UV protection that is optimized and increased by the impact of UV-B and UV-A radiation. The intensity of PAR modifies the plant's response to UV-B radiation. Thus, a spectral balance of PAR and UV radiation seems to be crucial for a changed profile of flavonoid accumulation, which is important not only in laboratory experiments but is also most likely an acclimation factor in the field.

Acknowledgements This work was supported by the Bavarian State Ministry of Sciences, Research, and the Arts in the program BayForUV.

Conflict of interest The authors declare that they have no conflict of interest.

References

Berkelaar EJ, Omrod DP, Hale BA (1994) The influence of photosynthetically active radiation on the effects of ultraviolet-B radiation on *Arabidopsis thaliana*. Photochem Photobiol 64:110–116

Bieza K, Lois R (2001) An *Arabidopsis* mutant tolerant to lethal ultraviolet-B levels shows constitutively elevated accumulation of flavonoids and other phenolics. Plant Physiol 126:1105–1115

Bornman JF, Teramura AH (1993) Effects of ultraviolet-B radiation on terrestrial plants. In: Young AR, Björn LO, Moan J, Nultsch W (eds) Environmental UV photobiology. Plenum, New York, pp 427–471

Burchard P, Bilger W, Weissenböck G (2000) Contribution of hydroxycinnamates and flavonoids to epidermal shielding of UV-A and UV-B radiation in developing rye primary leaves as assessed by ultraviolet-induced chlorophyll fluorescence measurements. Plant Cell Environ 23:1373–1380

Caldwell MM (1971) Solar UV radiation and the growth and development of higher plants. In: Giese AC (ed) Photophysiology, vol 6. Academic, New York, pp 131–177

Caldwell MM, Flint SD (1994) Lighting considerations in controlled environments for nonphotosynthetic plant responses to blue and ultraviolet radiation. In: Tibbitts TW (ed) International Lighting in Controlled Environments Workshop. NASA-CP-95-3309, pp. 113–124

Caldwell MM, Bornman JF, Ballaré CL, Flint SD, Kulandaivelu G (2007) Terrestrial ecosystems, increased solar ultraviolet radiation, and interactions with other climate change factors. Photochem Photobiol Sci 6:252–266

Casati P, Walbot V (2003) Gene expression profiling in response to ultraviolet radiation in maize genotypes with varying flavonoid content. Plant Physiol 132:1739–1754

Cooley NM, Truscott HMF, Holmes MG, Attridge TH (2000) Outdoor ultraviolet polychromatic action spectra for growth responses of *Bellis perennis* and *Cynosurus cristatus*. J Photochem Photobiol B 59:64–71

Dunaeva M, Adamska I (2001) Identification of genes expressed in response to light stress in leaves of *Arabidopsis thaliana* using RNA differential display. Eur J Biochem 268:5521–5529

Flint SD, Caldwell MM (2003) Field testing of UV biological weighting functions for higher plants. Physiol Plant 117:145–153

Ghetti F, Herrmann H, Häder D-P, Seidlitz HK (1999) Spectral dependence of the inhibition of photosynthesis under simulated global radiation in the unicellular green alga *Dunaliella salina*. J Photochem Photobiol B 48:166–173

Giordano CV, Mori T, Sala OE, Scopel AL, Caldwell MM, Ballaré CL (2003) Functional acclimation to solar UV-B radiation in *Gunnera magellanica*, a native plant species of southernmost Patagonia. Plant Cell Environ 26:2027–2036

Glombitza S, Dubuis P-H, Thulke O, Welzl G, Bovet L, Götz M, Affenzeller M, Geist B, Hehn A, Asnaghi C, Ernst D, Seidlitz HK, Gundlach H, Mayer KF, Martinoia E, Werck-Reichhart D, Mauch F, Schäffner AR (2004) Crosstalk and differential response to abiotic and biotic stressors reflected at the transcriptional level of effector genes from secondary metabolism. Plant Mol Biol 54:817–835

Ibdah M, Krins A, Seidlitz HK, Heller W, Strack D, Vogt T (2002) Spectral dependence of flavonol and betacyanin accumulation in *Mesembryanthemum crystallinum* under enhanced UV radiation. Plant Cell Environ 25:1145–1154

Izaguirre MM, Scopel AL, Baldwin IT, Ballaré CL (2003) Convergent responses to stress. Solar ultraviolet-B radiation and *Manduca sexta* herbivory elicit overlapping transcriptional responses in field-grown plants of *Nicotiana longiflora*. Plant Physiol 132:1755–1767

Jansen MAK, Gaba V, Greenberg BM (1998) Higher plants and UV-B radiation: balancing damage, repair and acclimation. Trends Plant Sci 3:131–135

Jordan BR (1996) The effects of ultraviolet-B radiation on plants: a molecular perspective. Adv Bot Res 22:97–162

Kaffarnik F, Seidlitz HK, Obermaier J, Sandermann H, Heller W (2006) Environmental and developmental effects on the biosynthesis of UV-B screening pigments in Scots pine (*Pinus sylvestris* L.) needles. Plant Cell Environ 29:1484–1491

Krizek DT (2004) Influence of PAR and UV-A in determining plant sensitivity and photomorphogenic responses to UV-B radiation. Photochem Photobiol 79:307–315

Langebartels C, Schraudner M, Heller W, Ernst D, Sandermann H (2002) Oxidative stress and defense reactions in plants exposed to air pollutants and UV-B radiation. In: Inzé D, Van Montagu M (eds) Oxidative stress in plants. Taylor & Francis, London, pp 105–135

Mazza CA, Battista D, Zima AM, Szwarcberg-Bracchitta M, Giordano CV, Acevedo A, Scopel AL, Ballaré CL (1999) The effects of solar ultraviolet-B radiation on the growth and yield of barley accompanied by increased DNA damage and antioxidant responses. Plant Cell Environ 22:61–70

McKenzie RL, Aucamp PJ, Bais A, Björn LO, Ilyas M (2007) Changes in biologically-active ultraviolet radiation reaching the Earth's surface. Photochem Photobiol Sci 6:218–231

Meijkamp BB, Doodeman G, Rozema J (2001) The response of *Vicia faba* to enhanced UV-B radiation under low and near ambient PAR levels. Plant Ecol 154:137–146

Quaite FE, Sutherland BM, Sutherland JC (1992) Action spectrum for DNA damage in alfalfa lowers predicted impact of ozone depletion. Nature 358:576–578

Ries G, Heller W, Puchta H, Sandermann H, Seidlitz HK, Hohn B (2000) Elevated UV-B radiation reduces genome stability in plants. Nature 406:98–101

Rossel JB, Wilson IW, Pogson BJ (2002) Global changes in gene expression in response to high light in *Arabidopsis*. Plant Physiol 130:1109–1120

Rousseaux MC, Ballaré CL, Giordano CV, Scopel AL, Zima AM, Szwarcberg-Bracchitta M, Searles PS, Caldwell MM, Diaz SB (1999) Ozone depletion and UVB radiation: Impact on plant DNA damage in southern South America. Proc Natl Acad Sci USA 96:15310–15315

Ryan KG, Markham KR, Bloor SJ, Bradley JM, Mitchell KA, Jordan BR (1998) UVB radiation induced increase in quercetin : kaempferol ratio in wild-type and transgenic lines of *Petunia*. Photochem Photobiol 68:323–330

Ryan KG, Swinny EE, Winefield C, Markham KR (2001) Flavonoids and UV photoprotection in *Arabidopsis* mutants. Z Naturforsch 56c:745–754

Ryan KG, Swinny EE, Markham KR, Winefield C (2002) Flavonoid gene expression and UV photoprotection in transgenic and mutant *Petunia* leaves. Phytochemistry 59:23–32

Sancar A (1994) Structure and function of DNA photolyase. Biochemistry 33:2–9

Schnitzler J-P, Jungblut TP, Heller W, Köfferlein M, Hutzler P, Heinzmann U, Schmelzer E, Ernst D, Langebartels C, Sandermann H (1996) Tissue localization of u.v.-B-screening pigments and of chalcone synthase mRNA in needles of Scots pine seedlings. New Phytol 132:247–258

Schnitzler J-P, Langebartels C, Heller W, Liu J, Lippert M, Döhring T, Bahnweg G, Sandermann H (1999) Ameliorating effect of UV-B radiation on the response of Norway spruce and Scots pine to ambient ozone concentrations. Global Change Biol 5:83–94

Stapleton AE (1992) Ultraviolet radiation and plants: burning questions. Plant Cell 4:1353–1358

Sullivan JH, Gitz DC III, Liu-Gitz L, Xu C, Gao W, Slusser J (2007) Coupling short-term changes in ambient UV-B levels with induction of UV-screening compounds. Photochem Photobiol 83:863–870

Thiel S, Döhring T, Köfferlein M, Kosak A, Martin P, Seidlitz HK (1996) A phytotron for plant stress research: how far can artificial lighting compare to natural sunlight? J Plant Physiol 148:456–463

Turunen M, Heller W, Stich S, Sandermann H, Sutinen M-L, Norokorpi Y (1999) The effects of UV exclusion on the soluble phenolics of young Scots pine seedlings in the subarctic. Environ Pollut 106:219–228

Weatherhead EC, Andersen SB (2006) The search for signs of recovery of the ozone layer. Nature 441:39–45

Yao Y, Yang Y, Ren J, Li C (2006) UV-spectra dependence of seedling injury and photosynthetic pigment change in *Cucumis sativus* and *Glycine max*. Environ Exp Bot 57:160–167